Shock Wave/Turbulent Boundary-Layer Interactions in Rectangular Channels

DANIEL C. REDA* AND JOHN D. MURPHY†
NASA Ames Research Center, Moffett Field, Calif.

Nomenclature

M = Mach number
p = pressure
Re_∞ = freestream unit Reynolds number
$Re_{\delta_0^*}$ = Reynolds number based on δ_0^*
T = temperature
W = channel span
x, y, z = coordinate system, see Fig. 1
x_i = shock intercept with test surface in the absence of any boundary layer
α = shock generator angle of attack
δ = boundary-layer thickness
δ^* = displacement thickness
θ = momentum thickness

Subscripts
$0, F$ = at start, end, of the interaction pressure rise
t = tunnel stagnation value, upstream of nozzle
w = wall

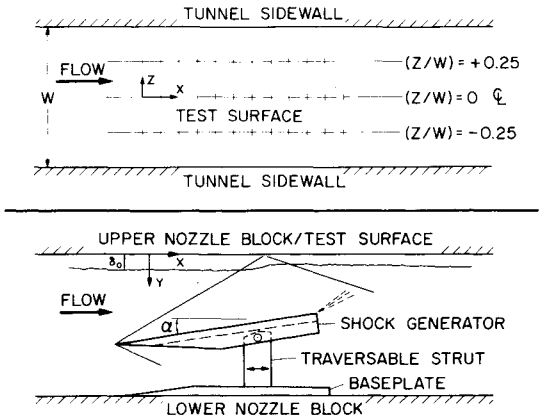

Fig. 1 Schematic of shock generator and instrumentation locations.

Theme

THE objective of this research was to experimentally investigate the interactions between incident oblique shock waves and turbulent boundary layers. Interaction regions were created by impinging full span, externally generated, shock waves on a nozzle wall boundary layer; the shock generator system was designed to meet previously reported criteria such that the resulting flowfields would be two-dimensional. Significant departures from two-dimensionality were observed over the entire range of shock strengths tested, and were identified with sidewall and corner boundary-layer effects. Comparisons of present centerline results with published two-dimensional data, obtained under similar test conditions and geometrical constraints, showed excellent agreement. This raises some question concerning the degree of two-dimensionality achieved in these previous investigations.

Contents

A recent survey article by Green[1] serves to outline the unresolved aspects of this phenomenon. One long standing controversy[2] has focused on the scale of the interaction region as a function of the over-all pressure rise across it. Hammitt[3] has demonstrated that experimental configuration is an important variable in shock wave/boundary-layer interactions, but the mechanism whereby configuration exerts its influence has not been determined. The present study was undertaken to further clarify these issues.

Tests were conducted in the 20.32 cm by 20.32 cm asymmetric, variable Mach number, supersonic tunnel of the NASA Ames Unitary system. Test conditions were: $M_0 = 2.9$, $P_t = 6.80$ atm, $T_t = 291\,^\circ$K, $(T_w/T_t) \simeq 1$ and $Re_\infty = 5.73 \times 10^7$/m. Schematics of the shock generator and test surface are shown in Fig. 1.

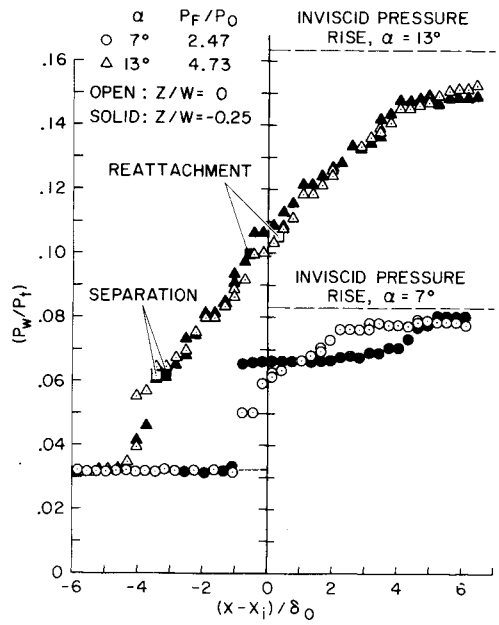

Fig. 2 Surface static pressure distributions, $\alpha = 7°$ and 13°.

Presented as Paper 72-715 at the AIAA 5th Fluid and Plasma Dynamics Conference, Boston, Mass., June 26–28, 1972; submitted July 11, 1972; synoptic received August 21, 1972. Full paper available from AIAA Library, 750 Third Avenue, New York, N.Y. 10017. Price: Microfiche, $1.00; hard copy, $5.00. **Order must be accompanied by remittance.**

Index categories: Boundary Layers and Convective Heat Transfer—Turbulent; Nozzle and Channel Flow; Jets, Wakes, and Viscid-Inviscid Flow Interactions.

* National Research Council Postdoctoral Research Associate. Member AIAA.

† Research Scientist. Member AIAA.

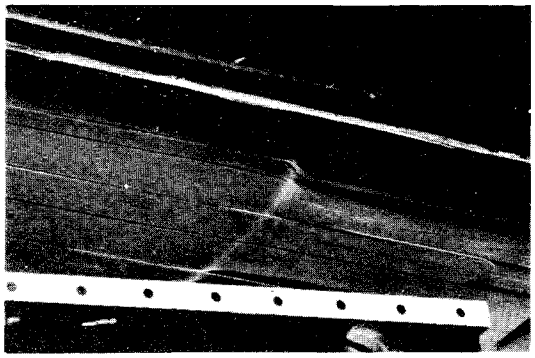

Fig. 3 Test surface oil flow pattern, $\alpha = 7°$.

Tunnel empty measurements showed the test boundary layer to be spanwise uniform, with $\delta_0 = 1.694$ cm, $\delta_0{}^* = 0.388$ cm, and $\theta_0 = 0.0817$ cm; no spanwise or axial pressure gradients were detected in the absence of an impinging shock wave. The ratio (W/δ_0) was 12/1; the sidewall boundary layers were those which developed naturally, and they were not deliberately altered in any manner.

Figure 2 shows wall pressure distributions representative of those measured throughout unseparated and separated interactions. At lower incident shock strengths, e.g., $\alpha = 7°$, centerline pressure distributions rose monotonically from the initial level to final levels closely matching those dictated by inviscid theory. Off centerline distributions did not coincide with those measured on centerline. Rather, they were characterized by a steeper initial pressure rise, followed by a plateau; final pressure levels were in agreement with those reached on centerline. These distributions implied an inflow or flow convergence near shock impingement.

As incident shock strength was increased, pressure distributions tended towards spanwise uniformity. For well separated flows, e.g., $\alpha = 13°$, the scale of the interaction region was increased, both on and off centerline pressure distributions exhibited a change in slope near separation, and the over-all pressure levels were somewhat below inviscid levels.

Figures 3 and 4 show oil flow photographs corresponding to the pressure distributions of Fig. 2 (flow is left to right). These patterns were photographed during steady-state run conditions, along a line of sight which originated below and slightly upstream of the test section window. For the unseparated interactions, a single ridge of oil formed, slightly

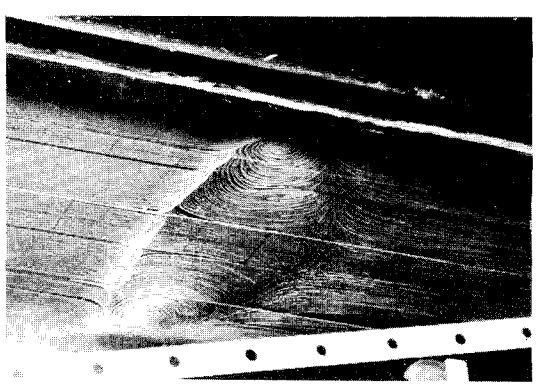

Fig. 4 Test surface oil flow pattern, $\alpha = 13°$.

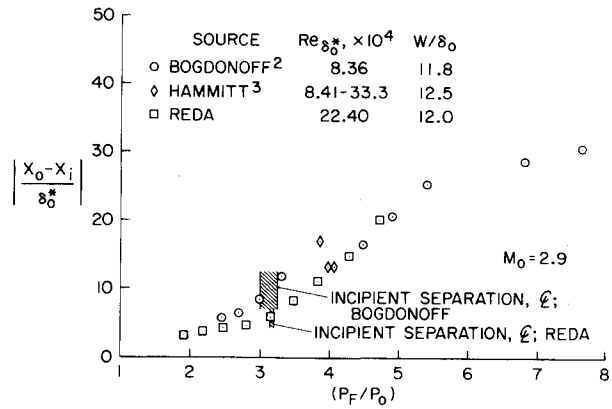

Fig. 5 Upstream influence vs over-all pressure rise.

concave, upstream facing. Definite flow convergence was observed in the vicinity of shock impingement.

This degree of flow convergence increased with increasing shock strength, until small regions of reverse flow formed on either side of centerline. These separated flow regions eventually merged at the channel centerline; once this occurred, the reversed flow region grew rapidly in streamwise dimensions for each additional increment in shock strength. Despite the existence of spanwise uniform pressure distributions, surface oil flow patterns for the well-separated interactions exposed some significant departures from two-dimensionality. The separation line was observed to be straight over the center half span. Inflow from the corners was seen to drive a pair of large standing vortices within the reverse flow region. The reattachment line was extremely concave, upstream facing. Sidewall oil flow patterns revealed that separation had occurred in the sidewall boundary layers as the incident shock sliced diagonally through them. Low energy air under these boundary layers was thereby swept upwards, into the corners of the channel, then laterally, into the reverse flow region.

Having established the mechanism for these departures from mean flowfield two-dimensionality, present centerline results were compared to published two-dimensional data. For example, Fig. 5 shows a comparison with the results of Refs. 2 and 3, for upstream influence vs over-all pressure rise. Note that all of these interactions were generated on nozzle wall boundary layers, in rectangular facilities of (W/δ_0) ratios near 12/1.

Similar levels of agreement were found with published data for incipient separation pressure levels, pressure rises to separation, wall pressure distributions, and scale of the interaction regions as a function of Reynolds number. Such agreement strongly suggests that these previously reported interactions suffered similar departures from two-dimensionality.

References

[1] Green, J. E., "Interactions Between Shock Waves and Turbulent Boundary Layers," *Progress in Aerospace Sciences*, Vol. 11, Pergamon Press, Oxford, 1970, pp. 235–340.

[2] Bogdonoff, S. M., Remarks on "Interactions Between Wholly Laminar or Wholly Turbulent Boundary Layers and Shock Waves Strong Enough to Cause Separation," *Journal of Aeronautical Sciences*, Vol. 21, Feb. 1954, pp. 138–139.

[3] Hammitt, A. G. and Hight, S., "Scale Effects in Turbulent Shock Wave Boundary Layer Interaction," AFOSR TN 60-82, *Proceedings of 6th Midwestern Conference on Fluid Mechanics*, Univ. of Texas, Austin, Sept. 1959.